CHARACTERIZATION TESTING OF A 40 AHR BIPOLAR NICKEL-HYDROGEN BATTERY

Jeffrey C. Brewer
NASA Marshall Space Flight Center
Huntsville, Alabama 35812

Michelle A. Manzo
NASA Lewis Research Center
Cleveland, Ohio 44135

Russel P. Gemeiner
NASA Lewis Research Center
Cleveland, Ohio 44135

Extensive characterization testing has been done on a second 40 amp-hour (Ahr), 10-cell bipolar nickel-hydrogen (Ni-H_2) battery to study the effects of such operating parameters as charge and discharge rates, temperature, and pressure, on capacity, Ahr and watt-hour (Whr) efficiencies, end-of-charge (EOC) and mid-point discharge voltages. Testing to date has produced many interesting results, with the battery performing well throughout all of the test matrix except during the high-rate (5C & 10C) discharges, where poorer than expected results were observed. The exact cause of this poor performance is, as yet, unknown. Small scale 2" x 2" battery tests are to be used in studying this problem.

Low earth orbit (LEO) cycle life testing at a 40% depth of discharge (DOD) and 10°C is scheduled to follow the characterization testing.

INTRODUCTION

Space power systems of the future are projected to require power levels that extend far beyond the current levels of demand. In order to meet these increasing needs, improvements must be made to current energy-producing systems or new technologies must be developed. Over the past several years, LeRC has been actively engaged in the development of a bipolar configured Ni-H_2 battery. This battery system has the potential to meet some of these high-power needs of the future. In a continuing effort to develop this technology to a point where it can be used efficiently in space flight, LeRC has begun testing a second 40 Ahr, 10-cell bipolar Ni-H_2 battery.

Results from the tests on the first battery tested here at LeRC were very encouraging. The battery operated for some 10,000 LEO cycles at 40% DOD and produced promising results in most of a variety of characterization tests, as well (ref. 1). Following the completion of this test, work began on the design of the second bipolar battery in hopes of developing an improved battery.

BATTERY DESIGN

The basic design of this battery differs from that of the first battery only through slight modifications in the cell frames. Poor high-rate discharge performance and electrolyte leakage paths in the first battery led to these changes. It was thought, at the time, that a possible cause of the poor high-rate performance in the first battery was limited gas access to the reaction sites on the negative electrode. Gas-access area was thus increased by modifying the cell frame in an attempt to alleviate this problem. The gaskets were also changed in the cell frame design in an effort to improve the seals and thus better contain the electrolyte within the cells. In addition to these minor design changes, most of the individual components of the second battery came from different manufacturers (table I). The reasons vary as to why these component changes were made. The frame material, for instance, was changed from polysulfone to ABS (resins which are terpolymers of acrylonitrile, butadiene, and styrene) because of superior machining capabilities and mechanical stability of the material. The nickel electrode was changed simply because of availability. The other changes were based, at least in part, on more technical reasoning and on the desire to reduce the number of parts. Because of inconsistencies found in the previous H_2 electrode, Giner, Inc. was engaged in a development program to manufacture a suitable large area, single unit electrode for this application. In doing so, the previous three-piece electrode would be eliminated. A program was also undertaken with National Standard to develop a fibrex electrolyte reservoir plate (ERP) which would contain pores in the desired range and could be manufactured in one piece. The previous ERP was constructed from nickel foam from Brunswick which, due to the large area required and manufacturing limitations, resulted in a six-piece ERP. In an attempt to increase the effective current carrying area between the gas screen and the bipolar plate and to improve high rate performance, the gas screen was changed to a heavier, woven screen, as opposed to an expanded metal (Exmet) screen in the first battery. This change also created a large weight increase which makes it difficult to justify its use without major performance improvements. Finally, the electrolyte concentration was changed from 31% to 26% potassium hydroxide. This was done because of superior life seen in IPV Ni-H_2 testing (ref. 2). These multiple component changes, as well as different testing procedures and unique cell characteristics make it difficult to directly compare results from the two batteries. Some comparisons, however, are valid and will be made.

One feature consistent with the first battery is that both utilized an active cooling process. This is accomplished by pumping a coolant through alternate bipolar plates (cooling plates) in the battery stack. This enables temperature readings to be controlled very consistently and accurately throughout the entire cell. This is one advantage over IPV technology. In an IPV cell, temperatures in the stack can run 7°C hotter than the measured temperatures outside the cell (ref. 3).

PROCEDURES

After construction was complete, the battery was placed in a boiler plate pressure vessel, which was designed to meet safety requirements. Each cell was

instrumented with voltage leads to measure individual cell voltages as well as a thermocouple attached to the bipolar plate in the hydrogen cavity to measure internal cell temperature. Additional thermocouples were placed on the exterior of the stack to get additional temperature measurements. The pressure vessel was equipped with a pressure transducer for measuring the hydrogen pressure, an oxygen sensor, and a relative humidity indicator. A Modicon programmable controller was used to run the test. All instrumented points were scanned and digitized every 18 seconds by a Neff multiplexer and stored by a central computer system for subsequent processing. The data could then be processed and received in both tabular and graphical form for each cycle.

Following the setup and checkout of the test hardware and data collection system, initial cycles were run to determine battery capacity. An initial capacity of 40 Ahrs was assumed. The capacity determination cycles basically consisted of a C/2 rate charge with a 5% overcharge followed by a C rate discharge to a battery voltage of 7.0 V or a low cell voltage of 0.5 V. "C" is defined as the rate at which the battery's capacity will be depleted in one hour. The low cell voltage cut-off of 0.5 V was used in order to prevent any cell from going negative and thus generating hydrogen. A C/4 drain to these same cut-off points followed this to complete the total cycle. As the cycles continued, the "C" value was adjusted several times until a consistent capacity was recorded, which was 40 Ahrs. While some of the formation cycles were run at 20°C and 200 psi, the baseline capacity determination cycles were run at 10°C and 200 psi.

Characterization tests were then run at a variety of charge and discharge rates, temperatures, and pressures. A full set of tests was run at 10°C and 200 psi at charge rates of C/4, C/2, and C, and discharge rates of C/4, C/2, C, 2C, 5C, 10C, and 5C pulse for each charge rate. Following this set of tests, subsets of this base characterization test were run at other temperatures and pressures. A C/2 rate charge was chosen as the charge rate to be used in these subsets. This selection was based not only on performance in the base characterization test, but also on performance in prior tests (ref. 4). A C/2 rate charge also allowed the cycles to fit better into an eight-hour day than if run at a lower rate. A subset of tests run at 20°C and 200 psi consisted of the identical discharge rates used in the base set paired with the C/2 charge rate. The remaining subsets (0°C at 200 psi, 30°C at 200 psi, and 20°C at 400 psi) consisted only of the C/4, C/2, C, and 2C rate discharges. Again, all were paired with the C/2 charge rate. Each individual test was run until three consistent cycles were recorded. Consistency was based on Ahr and Whr efficiencies. Each cycle consisted of a full charge (the amount of which was equal to the capacity out in the preceding discharge plus a set percentage of overcharge) followed by a full discharge to a battery voltage of 7.0 V or a low cell voltage of 0.5 V (hereafter known as the normal cut-off points). A C/4 drain followed all discharges run at a C/2 rate or higher.

A set percentage of overcharge was used in this test in order to ensure adequate charging as well as protect from unnecessary overcharging. This is compared to the first battery test where a set charge input was used for each cycle regardless of the capacity delivered in the previous discharge (ref. 1). A 5% overcharge was used initially; however, this proved to be insufficient to adequately recharge the battery so the overcharge was increased to 10%. This percentage maintained a stable capacity from cycle to cycle; however, to reduce

any unnecessary overcharging, the percentage was dropped to 7% where stable capacities were once again realized. The overcharge amount thus stayed at 7% throughout the remainder of the characterization testing.

Due to a lack of adequate manpower, cycles were not run over the weekends or holidays. This extended wet-stand period allowed time for a weak, high-resistance cell to self-discharge considerably more than the other cells. This delayed the resuming of the characterization testing until after that cell could be brought back up to a state of charge similar to that of the other cells. It was found through trial and error that the weak cell could be maintained by trickle charging the fully charged battery at a C/150 to C/100 rate. This method produced much more consistent results than other methods that were tried and allowed characterization cycles to resume much more quickly.

RESULTS AND DISCUSSION

Due to the wide range of variables in this test, all of the relevant numerical data will not be enumerated here, but is summarized in tables II - VIII. Figures 1 - 4 contain pertinent voltage profiles from throughout the test.

Before discussion can begin on the specific results in the test, a general point needs to be made concerning the data to be discussed hereafter. It was mentioned earlier about the problems caused by a weak cell during extended wet-stand periods. This same weak cell created problems during the characterization cycles, as well. The discharges on most, if not all, of the early characterization cycles were terminated by a battery voltage of 7.0 V. This allowed good, accurate comparisons of data from cycle to cycle. The discharges, however, on the vast majority of characterization cycles were terminated by a low cell voltage of 0.5 V, while the overall battery voltage ranged from 7.1 to 10.4 V. Because most of the cycles thus had no common end-of-discharge (EOD) point, it was difficult to compare the basic, overall data between cycles. So, where it was helpful, capacity delivered to the 10.0 V point in the discharges was used to compare cycles in hopes of negating some of the distorting effects of the weak cell on the normal cut-off point data. Just what caused this cell to perform this way is unknown at this time; however, it is thought that shunt currents could be present which allowed an additional discharge path through which the cell self-discharged over night between cycles. This would explain the erratic behavior seen throughout the characterization cycles.

One additional comment about the data -- each data point represents the average value of the three most consistent cycles run at that particular set of test conditions.

Increasing the charge rate had little consistent effect on the capacity delivered to the normal cut-off points, although at lower charge rates the battery seemed to perform slightly better. Even the capacity delivered to 10.0 V showed no consistent trends (table II). Increasing the charge rate also had little consistent effect on the Ahr efficiency, but, due to the accompanying increase in battery charge voltage from an average of 15.52 V at the C/4 rate to 16.65 V at the C rate, caused an average decrease of 7.3% in the Whr efficiency, except

at the 2C rate discharge where no significant changes were seen (table III). Thus, because of its desirable effect on Whr efficiency and lack of effect on other variables, a low charge rate would seem to be best; however, previous testing has suggested that a C/2 to C charge rate range should produce the optimum results (ref. 4). It is difficult, however, to directly compare results from this characterization test with the referenced test due to the fact that the nickel electrodes used in both tests came from different manufacturers. Electrolyte concentration was also different. These differences alone could account for the discrepancies seen between the two tests. In either case, though, results failed to show strong proof that there is clearly an optimum charge rate.

Increasing the discharge rate caused a consistent decrease in the capacity delivered over all temperatures and pressures except at 20°C and 400 psi where the capacity increased slightly from 46.03 Ahr to 47.46 Ahr at discharge rates of C/4 and C/2, respectively (table IV). The probable cause of this apparent increase in capacity delivered at the higher rate can be traced to the weak cell causing an early termination of the discharges run at the lower rate. Comparing the capacities at the 10.0 V point in the discharge supports this theory. At 10.0 V, an average capacity of 43.99 Ahr was delivered at the C/4 rate and 42.59 Ahr was delivered at the C/2 rate.

Because of the lower capacities delivered at the higher discharge rates, the resulting Ahr efficiencies also decreased across the board (table V). Also, as discharge rates increased, Whr efficiencies decreased over all temperatures and pressures due to the decrease in operating voltages that always accompany increasing discharge rates (tables VI & VII). In this report, operating voltages are reported as mid-point discharge voltages, which were calculated by averaging the following two data points: the voltage reading at 1/2 of the total discharge time and the voltage reading at the 20 Ahr out point. Discharge voltage profiles vs. capacity at all discharge rates can be seen in figure 1.

The discharge rate effects were all as anticipated; however, at high discharge rates of 5C and 10C, performance was very poor. Poor performance was also seen at these rates in the first battery (ref. 1); but, despite attempts to alleviate this problem through design and individual component changes, even poorer performance was seen in the second battery (figure 2). In the attempts to run a 10C discharge, the battery voltage dropped below 7.0 V within 30 seconds. Another 10C discharge was run and was allowed to continue past the normal cut-off points down to a low cell voltage of 0.1 V. This discharge lasted 3 minutes but the voltage did not begin to level off until around 4.5 V (figure 1). The 5C discharges lasted longer but, again, failed to level off above a battery voltage of 7.0 V. (tables IV - VI and figure 1). Only a 5C pulse (1 second on / 4 seconds off) discharge was able to produce meaningful results (tables IV & V and figures 1 & 3).

Several ideas have been discussed as to what could be causing this high-rate discharge problem. Limited gas access to the negative electrode was previously mentioned as a possible cause. The design changes mentioned earlier that were made in an attempt to alleviate this problem instead could have elevated the problem even more. This is based on the possibility that the holes drilled in the battery frame to allow gas access into the interior of the battery became

filled with electrolyte and blocked free gas flow. One argument against this scenario is that the pressure of the gas flowing to and from the electrodes would keep the holes clear. Also, if gas access is the problem, then, based on the amount of H_2 located in the cavity adjacent to the negative electrode, initial voltage performance might be expected to be good but would fall off as the H_2 gas located in the cavity was used up. Data from the high-rate discharges showed no signs of good initial voltage performance and even showed signs of leveling off at a low voltage. A second possible cause is poor contact between the gas screen and the two surrounding components -- the negative electrode and the bipolar plate. Due to the large surface area of the bipolar stack components, uniform stack compression and the resulting surface contact between individual components is difficult to consistently maintain. A lack of adequate contact area would limit the current carrying capability and produce poor results especially at high current levels. Another possible cause is the Goretex backing placed on the H_2 electrode during the standard production process at Giner, Inc. Its presence could possibly be limiting the effective contact area between the H_2 electrode and the gas screen, thus hindering current flow. There was some initial concern about the possibility that this backing could cause current flow problems in a bipolar configuration; however, polarizations of up to 500 mA/cm^2 were operated successfully on a small scale prior to construction of the full size electrode. Perhaps the key point, once again, is the possible lack of uniform stack compression in a full scale battery configuration. One possible solution that has been discussed that could, at least, partially improve the contact between components is to weld the gas screen to the bipolar plate. This would assure adequate contact area between these two components, but would not improve the contact area between the H_2 electrode and the gas screen. The effects on performance that the Goretex backing has in a full scale battery as well as other possible problem areas are to be addressed in further testing. Small scale 2" x 2" battery tests will begin soon and will be used to evaluate some of these areas. Flooded capacity tests have already been done to evaluate the performance effects caused by varying the nickel electrode manufacturer and the electrolyte concentration. Electrodes from both manufacturers (Eagle Picher and Whittaker-Yardney) were tested at 10C, 5C, 2C, C, C/2, and C/4 discharge rates using 26, 31, and 40% KOH as electrolyte. Nickel was used as the counter electrode and amalgamated zinc was used as the reference electrode. Results from this test showed no signs of inferior high-rate performance by the Whittaker-Yardney nickel electrode used in the second battery (figure 4). On the contrary, these electrodes produced much more stable efficiencies and capacities at all discharge rates tested (table VIII). The Whittaker-Yardney electrodes shown in table VIII produced 76% of their low-rate (C/4) capacity at the high (10C) rate, while the Eagle Picher electrodes delivered only 39% of their low-rate capacity at the high rate. It is not possible, however, to completely rule out the nickel electrode as being responsible for the poor high-rate discharge performance. Because of the flooded conditions under which these capacity measurements were made, the ability of the different electrodes to perform under actual battery conditions was not addressed. Thus, it is entirely possible that under actual battery conditions the Whittaker-Yardney electrodes would not perform optimally and that the "starved" condition could lead to the type of poor performance that was seen at the high rates. Finally, it was not intended through these tests to directly compare the two manufacturers' electrodes. Neither manufacturer optimized the electrodes that were used; they simply supplied standard electrodes of the size requested.

Temperature variations between 0°C and 30°C produced some interesting results. As expected, an increase in temperature produced significant drops in EOC voltage due to the decrease in internal resistance that accompanies rising temperatures. Readings averaged 16.40 V at 0°C and 15.12 V at 30°C. As temperatures increased, the mid-point discharge voltages, however, showed a steady increase at all discharge rates except at C/4 where a 50 mV drop was seen between the temperatures of 0°C and 10°C. (table VII). The improved voltage performance seen at higher temperatures, however, did not directly translate into an increase in Whr efficiencies at all conditions (table VI). At the 2C rate discharge the Whr efficiency was the lowest (41.26%) at 30°C and the highest (53.43%) at 20°C. At the other three discharge rates, though, 30°C produced the highest efficiencies. The discrepancy at the 2C rate discharge can be, at least partially, attributed to a high EOD voltage of 10.3 V at 30°C compared to 7.2 V at 20°C. Whether or not the large percentage difference could have been completely overcome had the 30°C discharge run down to around 7.0 V is difficult to determine; but, certainly a large portion of it would have been. The effect that temperature had on total capacity out was equally interesting. For instance, as temperatures increased from 0°C to 20°C, capacity delivered to the normal cut-off points increased at the C/2 rate discharge from 41.19 Ahr to 47.68 Ahr, respectively, but fell off drastically at 30°C to 37.50 Ahr (table IV). This trend was consistent at all discharge rates and was also seen in the capacity data to the 10.0 V point in the discharge. Ahr efficiencies, however, seemed to be less consistently affected by temperature variations (table V). All of this data seems to support the use of temperatures as high as 20°C or even 30°C to produce optimum results. This agrees rather well with the data produced during the first battery test (ref. 1).

Increasing the H_2 pressure inside the vessel also produced some interesting results. Negligible change was seen in the EOC voltage between 200 and 400 psi as the voltage dropped from 15.62 V to 15.59 V, respectively; however, at 400 psi, an improvement was seen in the mid-point discharge voltage at all discharge rates (table VII). This was expected behavior because the increased pressure would increase the activity coefficient of the gas and thus improve its efficiency and voltage performance. When looking at the data measured to the normal cut-off points in the discharge, the capacity, and Ahr and Whr efficiencies all were less at the higher pressure, except at the C/4 rate discharge, where a slight increase in both Ahr and Whr efficiencies was seen (tables IV - VI). These were not expected results but, once again, the weak cell seems to be distorting the data by prematurely terminating the discharges during the 400 psi cycles. Although the capacity delivered to 10.0 V is still greater at 200 psi, the differences are not as great. Also, the Ahr and Whr efficiency differences can be reasonably eliminated by considering the high EOD voltages on the 400 psi cycles. Actually, the Whr efficiencies would have probably been greater at 400 psi had all discharges terminated at similar voltages. It certainly should illustrate that increasing or decreasing the pressure will have minimal effects on overall battery performance.

After completion of the characterization cycles, the battery was placed on LEO cycle life testing at 40% DOD and at 10°C.

CONCLUSIONS AND RECOMMENDATIONS

Despite the fact that a weak cell made it difficult to directly compare some of the data from cycle to cycle, there was enough evidence to see that the battery produced generally expected results and performed very well throughout the majority of the characterization test matrix. It is hoped and expected that the LEO cycle life test that has just begun will produce similarly encouraging results. One area that continues to be a problem, however, is the high-rate discharge performance of the battery. Even though improvements were not made in this area with this battery, several encouraging ideas have been mentioned as possible solutions to the poor high-rate performance problem. As mentioned earlier, several studies, including small scale 2" x 2" battery tests, will be done in hopes of pinpointing the area or areas responsible for the poor high-rate performance.

REFERENCES

1. Cataldo, R.L.: Parametric and Cycle Tests of a 40-A-hr Bipolar Nickel-Hydrogen Battery. 21st Intersociety Energy Conversion Engineering Conference, Vol. 3, pp. 1547-1553.

2. Lim, H.S.; and Verzwyvelt, S.A.: KOH Concentration Effect on the Cycle Life of Nickel-Hydrogen Cells. II. Accelerated Cycle Life Test. 21st Intersociety Energy Conversion Engineering Conference, Vol. 3, pp. 1601-1606.

3. Rogers, H.; Levy, Jr., E.; Stadnick, S.J.; and et al: Failure Mechanisms in Nickel-Hydrogen Cells, Final Report. December 1977, pg. 2-36.

4. Cataldo, R.L.: Test Results of a Ten Cell Bipolar Nickel-Hydrogen Battery. 18th Intersociety Energy Conversion Engineering Conference, Vol. 4, pp. 1561-1567.

Table I. - COMPONENT DIFFERENCES BETWEEN BATTERY 1 AND BATTERY 2

Component	Battery 1	Battery 2
Frame	Polysulfone - Old	ABS - New
Nickel electrode	Eagle Picher	Whittaker - Yardney
Hydrogen electrode	LSI	Giner
ERP	Ni foam - Brunswick	Ni felt - Nat'l Std
Gas screen	Exmet	Woven (Nat'l Std)
Separator	Asbestos	Asbestos
Electrolyte	31% KOH	26% KOH

Table II. - CHARGE RATE EFFECTS ON CAPACITIES DELIVERED TO NORMAL CUT-OFF VOLTAGES & TO 10.0 VOLTS AT 10°C AND 200 PSI; BATTERY EOD VOLTAGES SHOWN UNDER NORMAL CUT-OFF CAPACITY VALUES

Discharge Rate	Capacity to Normal Cut-offs			Capacity to 10.0 V		
	Charge rate			Charge rate		
	C/4	C/2	C	C/4	C/2	C
C/4	47.45 7.0	46.90 6.9	46.87 7.0	43.15	42.85	43.06
C/2	46.80 7.0	46.12 6.8	43.72 7.1	42.60	42.02	40.34
C	41.73 7.1	42.38 7.3	40.84 8.0	37.75	39.08	38.97
2C	35.92 7.1	37.93 7.1	37.17 7.4	20.88	21.52	24.27

Table III. - CHARGE RATE EFFECTS ON AHR & WHR EFFICIENCIES AT 10°C AND 200 PSI

Discharge Rate	Ahr Efficiency, %			Whr Efficiency, %		
	Charge rate			Charge rate		
	C/4	C/2	C	C/4	C/2	C
C/4	94.16	93.60	93.77	80.16	78.17	74.45
C/2	87.76	86.30	85.95	72.43	69.21	66.20
C	76.99	77.04	75.76	60.43	58.93	55.83
2C	67.09	67.72	70.39	46.62	45.85	46.32

Table IV. - CAPACITY DELIVERED TO NORMAL CUT-OFF VOLTAGES AT ALL TESTED CONDITIONS WITH A C/2 RATE CHARGE; BATTERY EOD VOLTAGES SHOWN UNDER CAPACITY VALUES

Discharge Rate	Capacity, Ahr					
	200 psi				20°C	
	0°C	10°C	20°C	30°C	200 psi	400 psi
C/4	42.15 9.7	46.90 6.9	50.49 7.4	40.71 7.9	50.49 7.4	46.03 8.9
C/2	41.19 10.4	46.12 6.8	47.68 ***	37.50 7.3	47.68 ***	47.46 7.5
C	38.32 9.3	42.38 7.3	44.20 7.3	35.48 9.2	44.20 7.3	38.82 8.7
2C	33.17 7.6	37.93 7.1	39.45 7.2	32.60 10.3	39.45 7.2	33.66 9.0
5C	###	15.43 7.0	22.24 6.9	###	22.24 6.9	###
5C Pulse	###	30.60 7.0	33.97 8.1	###	33.97 8.1	###

*** - No readings available due to data collection system errors
- 5C and 5C Pulse run only at 10°C and 20°C at 200 psi

Table V. - AHR EFFICIENCIES AT ALL TESTED CONDITIONS WITH A C/2 RATE CHARGE

Discharge Rate	Ahr Efficiency, %					
	200 psi				20°C	
	0°C	10°C	20°C	30°C	200 psi	400 psi
C/4	90.80	93.60	92.04	90.96	92.04	92.55
C/2	85.79	86.30	86.76	86.68	86.76	86.20
C	82.80	77.04	78.86	79.62	78.86	76.85
2C	72.67	67.72	72.39	72.23	72.39	68.38
5C	###	28.18	41.52	###	41.52	###
5C Pulse	###	52.08	65.18	###	65.18	###

- 5C and 5C Pulse run only at 10°C and 20°C at 200 psi

Table VI. - WHR EFFICIENCIES AT ALL TESTED CONDITIONS WITH A C/2 RATE CHARGE

Discharge Rate	Whr Efficiency, %					
	200 psi				20°C	
	0°C	10°C	20°C	30°C	200 psi	400 psi
C/4	75.90	78.17	77.92	79.99	77.92	80.09
C/2	69.28	69.21	***	75.29	***	71.52
C	61.67	58.93	63.69	68.32	63.69	63.64
2C	46.51	45.85	53.43	41.26	53.43	52.91
5C	###	15.35	24.82	###	24.82	###

*** - No readings available due to data collection system errors
- 5C and 5C Pulse run only at 10°C and 20°C at 200 psi

Table VII. - MID-PT. DISCHARGE VOLTAGES AT ALL TESTED CONDITIONS WITH A C/2 RATE CHARGE

Discharge Rate	Mid-Pt. Discharge Voltage, V					
	200 psi				20°C	
	0°C	10°C	20°C	30°C	200 psi	400 psi
C/4	12.90	12.85	12.95	13.20	12.95	13.10
C/2	12.40	12.45	12.65	13.00	12.65	12.80
C	11.45	11.72	12.15	12.60	12.15	12.45
2C	9.70	10.15	11.10	11.83	11.10	11.55

Table VIII. - CAPACITIES & AHR EFFICIENCIES FOR FLOODED ELECTRODE TESTS

Discharge Rate	Capacity, Ahr		Ahr Efficiency, %	
	EP31	WY26	EP31	WY26
C/4	0.64	0.43	71.95	73.07
C/2	0.63	0.41	71.19	70.48
C	0.59	0.40	66.54	68.00
2C	0.55	0.39	61.92	67.43
5C	0.47	0.37	52.63	62.86
10C	0.25	0.33	28.20	56.90

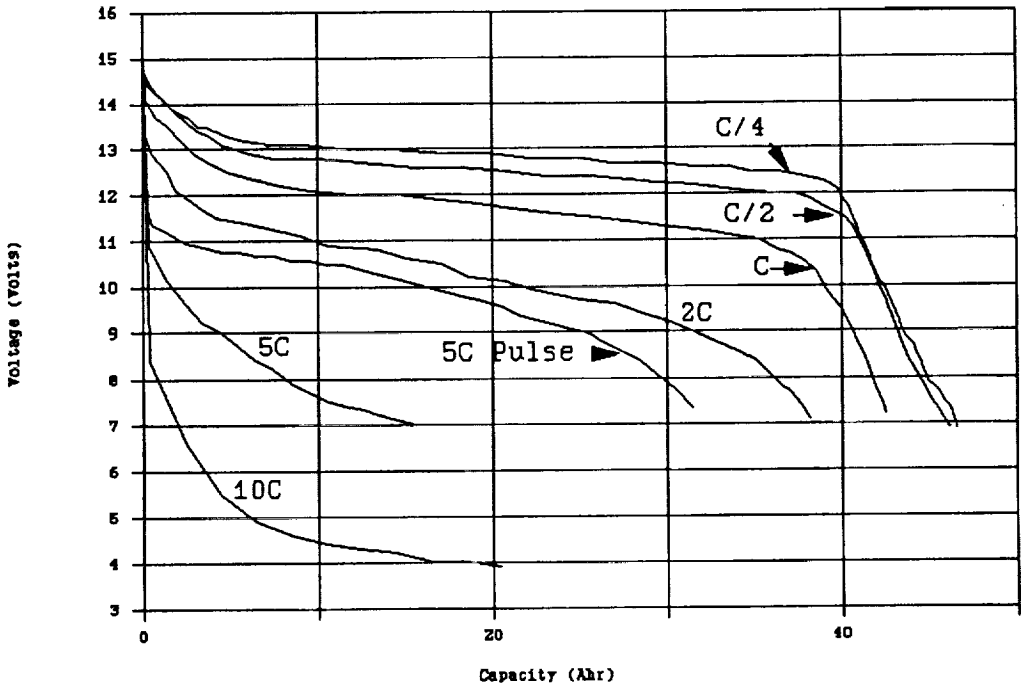

Figure 1. - Discharge voltage profiles vs. capacity for all discharge rates @ 10°C & 200 psi

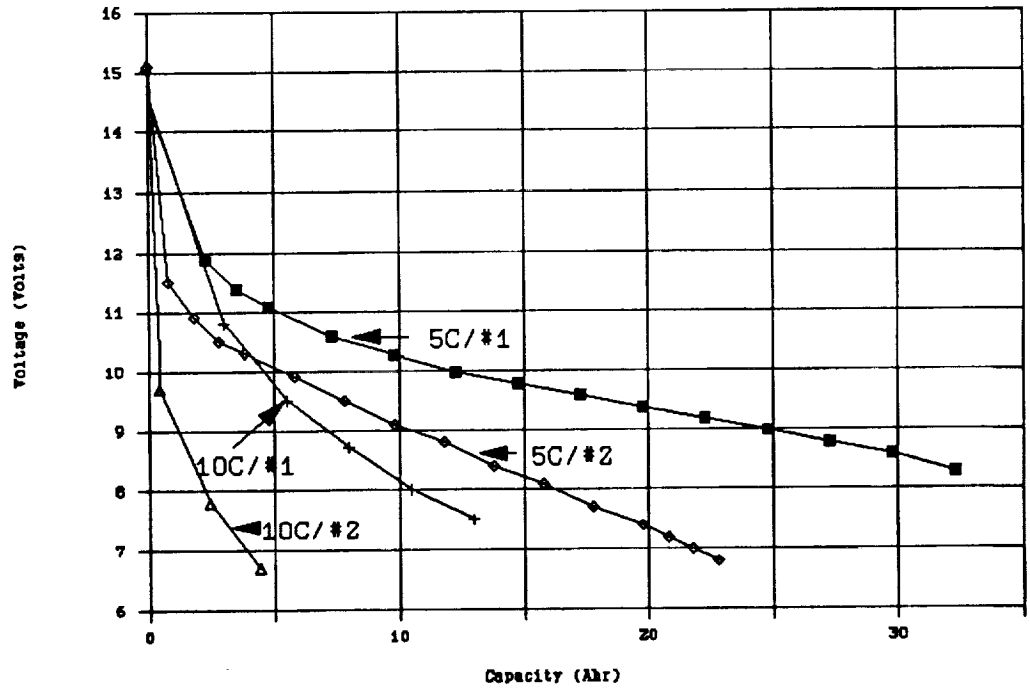

Figure 2. - 5C & 10C rate discharge voltage profile vs. capacity @ 20°C & 200 psi for battery 1 & battery 2

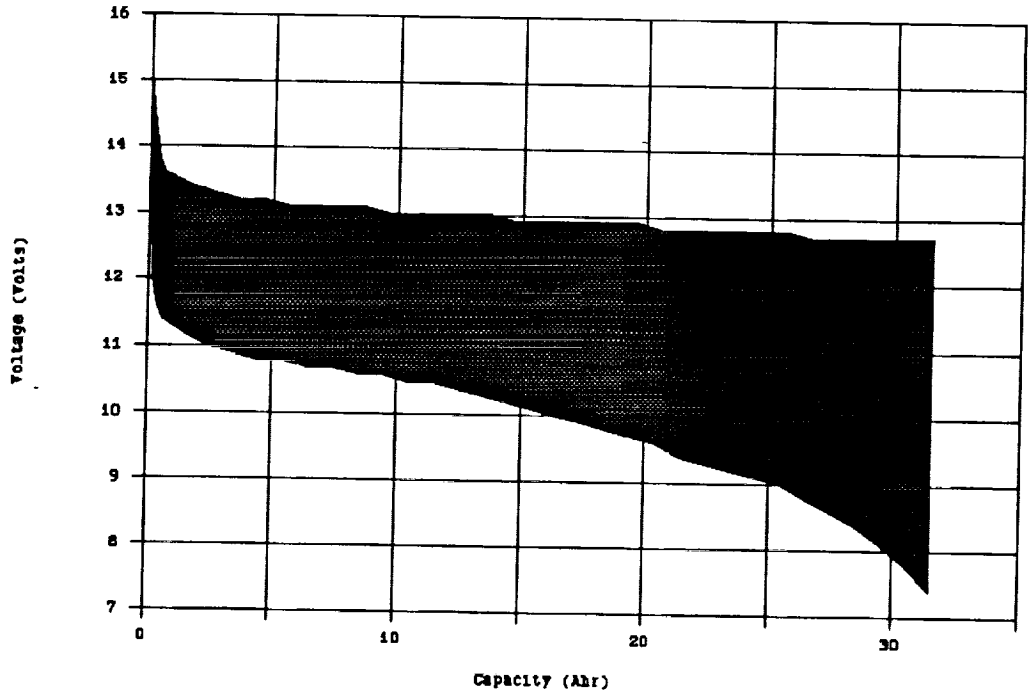

Figure 3. - 5C pulse (1 sec on / 4 sec off) discharge voltage profile vs. capacity @ 10°C & 200 psi

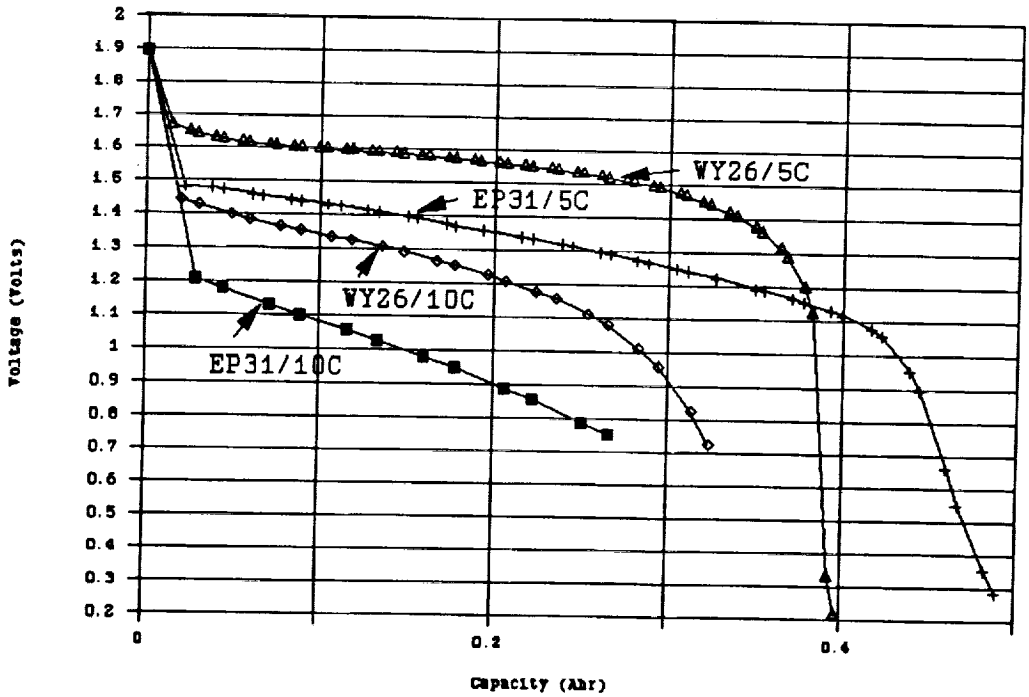

Figure 4. - 10C & 5C discharge voltage profiles vs. capacity during flooded electrode tests for Eagle Picher electrode in 31% KOH and Whittaker/Yardney electrode in 26% KOH